



## Defluoridation from aqueous solution by lanthanum hydroxide

Choon-Ki Na<sup>\*</sup>, Hyun-Ju Park

Department of Environmental Engineering, Mokpo National University, 61 Dorim, Chungkye Muan, Jeonnam 534-729, South Korea

### ARTICLE INFO

#### Article history:

Received 25 February 2010

Received in revised form 8 June 2010

Accepted 12 July 2010

Available online 21 July 2010

#### Keywords:

Defluoridation

Lanthanum hydroxide

Sorption isotherms

Kinetic modeling

Competing anions

Thermodynamic parameters

### ABSTRACT

This research was undertaken to evaluate the feasibility of lanthanum hydroxide for fluoride removal from aqueous solutions. A batch sorption experiments were conducted to study the influence of various factors such as pH, presence of competing anions, contact time, initial fluoride concentration and temperature on the sorption of fluoride on lanthanum hydroxide. The optimum fluoride removal was observed in the  $\text{pH}_{\text{eq}} \leq 7.5$ . The presence of competing anions showed no adverse effect on fluoride removal. The equilibrium data reasonably fitted the Langmuir isotherm model, and the maximum monolayer sorption capacity was found to be 242.2 mg/g at  $\text{pH}_{\text{eq}} \leq 7.5$  and 24.8 mg/g at  $\text{pH}_{\text{eq}} > 10.0$ . The pseudo-second-order kinetic model described well the kinetic data, and resulted in the activation energy of 53.4–68.8 kJ/mol. It was suggested that the overall rate of fluoride sorption is likely to be controlled by the chemical process. Thermodynamic parameters such as  $\Delta G^\circ$ ,  $\Delta H^\circ$  and  $\Delta S^\circ$  indicated that the nature of fluoride sorption is spontaneous and endothermic. The used lanthanum hydroxide could be regenerated by washing with NaOH solution. Results from this study demonstrate the potential usability of lanthanum hydroxide as a good fluoride selective sorbent.

© 2010 Published by Elsevier B.V.

### 1. Introduction

Fluoride in the environment occurs through natural presence in the earth's crust and industrial activities, especially, semiconductor, electroplating, coal fired power stations, aluminum, glass, ceramic and fertilizers industries [1,2]. The effluents of these industries have higher fluoride concentrations than natural waters, ranging from ten to thousands of mg/L [3]. The discharge of such wastewater leads to the fluoride contamination of surface and ground water. Fluoride is known as both beneficial and detrimental effect on human health. It is well known that fluoride can effectively prevent dental caries when a relative low level is constantly maintained in the oral cavity. On the contrary, an excessive fluoride intake leads to various diseases such as dental and skeletal fluorosis and non-skeletal fluorosis [4,5]. The optimum level of fluoride in drinking water for general good health is considered to be between 1.0 and 1.5 mg/L [6]. US EPA established a discharge standard of 4 mg/L for fluoride from wastewater treatment plant [7].

Various treatment technologies based on adsorption and biosorption [9–11], ion-exchange [12], chemical precipitation including electro-coagulation/flotation [13,14], and membrane processes, such as reverse osmosis [15], Donnan dialysis [16], nano-filtration [17], and electro-dialysis [18] have been suggested for fluoride removal. Most of these methods suffer from vari-

ous problems such as high operational and maintenance costs, low selectivity and capacity, secondary pollution and complicated procedure involved in the treatment. Comparatively, adsorption seems to be a more attractive method for the fluoride removal in terms of cost, simplicity of operation and selectivity. Numerous adsorbents like activated alumina [19], clay [8,20], hydroxyapatite [21], activated carbon [22], ion-exchange resin [23], quick lime [24], waste residue [25,26], and geomaterials [27–30] have been tested for fluoride removal. In recent years, rare earth element impregnation of porous adsorbents or carrier materials was found to be significantly effective for improving the selectivity and sorption of fluoride. For example, lanthanum-impregnated silica gel [31], lanthanum- and yttrium-impregnated alumina [32], lanthanum-impregnated chelating resins [33], lanthanum-loaded fiber [34], neodymium- and lanthanum-modified chitosan [35,36] have shown very promising results for fluoride removal from aqueous solutions.

The aim of this study is to understand the role of lanthanum for fluoride removal. In the present study, the sorption properties of lanthanum hydroxide,  $\text{La}(\text{OH})_3$  for fluoride removal from aqueous solution have been investigated in a batch mode. Sorption studies were conducted under various experimental conditions, such as contact time, initial fluoride concentrations, temperature, pH and the presence of competing anions. The experimental data were described with various isotherms and kinetic models generally adapted in the literatures to identify the adsorption mechanism. The possibility of lanthanum hydroxide for repeating use was also examined by a desorption study.

<sup>\*</sup> Corresponding author. Tel.: +82 61 450 2483; fax: +82 61 452 8762.  
E-mail address: [nack@mokpo.ac.kr](mailto:nack@mokpo.ac.kr) (C.-K. Na).

## 2. Experimental

### 2.1. Materials and reagents

Lanthanum hydroxide ( $\text{La}(\text{OH})_3$ , 99.9%) used as the sorbent for defluoridation experiments was purchased from Daejung Chemical Co., Korea. The lanthanum hydroxide used has a grain size range of 0.36–76.32  $\mu\text{m}$  (mean diameter 10.20  $\mu\text{m}$ ) and the specific surface area of 715.4  $\text{m}^2/\text{g}$ . The pH of point of zero charge ( $\text{pH}_{\text{pzc}}$ ) determined by the potentiometric titration method was between 8.7 and 8.8. A stock solution of fluoride (0.1 mol/L) was prepared by dissolving NaF (Sigma–Aldrich Co., USA) in deionized water and diluted to 0.002–0.008 mol/L as needed. The chemicals, NaCl,  $\text{NaHCO}_3$ ,  $\text{NaNO}_3$ ,  $\text{NaH}_2\text{PO}_4$ , and  $\text{Na}_2\text{SO}_4$  were used as the anion sources competing with fluoride ion in the working solution for sorption experiment. All reagents were of the highest grade available and were used as received. Polystyrene-based PA308 resin ( $-\text{N}^+(\text{CH}_3)_3\text{Cl}^-$ , Samyang Co., Korea) which is a strong base anion-exchange resin was used as a comparative sorbent.

### 2.2. Sorption experiments

Sorption experiments were carried out in batch conditions where 0.01–0.1 g of sorbent was added to 250 mL HDPE bottles containing 100 mL of working solution of known ion species and concentrations. The effect of different pH values on fluoride sorption was studied by adjusting the pH of solution using either 0.1 M HCl or 0.1 M NaOH solutions to the required pH range of 2.5–10.5. The bottles were settled in an incubator shaker and then continuously shaken at 120 rpm for a predetermined time period. The reaction temperature was set in the range of 25–45 °C. After the predetermined sorption time, solid and liquid phases were separated using 0.2  $\mu\text{m}$  membrane filter, fluoride concentrations in the liquid phase were measured. The sorption capacity,  $q$  (mg/g) was calculated using the following mass balance equation:

$$q = \frac{V(C_0 - C)}{W} \quad (1)$$

where  $C_0$  and  $C$  are the initial and final liquid-phase concentrations of fluoride (mg/L), respectively.  $V$  is the volume of solution (L) and  $W$  is the dry weight of sorbent used (g).

For desorption study, fluoride-loaded lanthanum hydroxide that was separated from solution by filtration after the sorption experiment was washed with deionized water and dried at 80 °C. 0.1 g of dried fluoride-loaded lanthanum hydroxide was placed in a HDPE bottle containing 20 mL of 0.1–2.0 M NaOH, and then shaken at 120 rpm for 1 h at 25 °C. The final concentration of fluoride in the desorption medium separated by filtration was determined using ion chromatography. The percentage of desorption was calculated from the amount of fluoride-loaded on lanthanum hydroxide and the final concentration of fluoride in the desorption medium.

### 2.3. Analysis

The concentration of fluoride and other anions in the solution were determined by single-column ion chromatography (Waters LC, USA) assembled with a 50  $\mu\text{L}$  injection loop, analytical column (Waters IC-pak A, 4.6 mm  $\times$  50 mm), suppressor module (Alltech model 335 SPCS), conductivity detector (Waters 432), and data module (Autochro-Win, Young-in Instrument Co., Korea). The pH of the solutions was measured using an Orion 3-Star bench-top pH meter (Thermo Fisher Scientific Inc., USA). The point of zero surface charge ( $\text{pH}_{\text{pzc}}$ ) value of the lanthanum hydroxide was estimated by the potentiometric titration method as described [37]. The surface area and particle size of the lanthanum hydroxide used were analyzed by a TriStar II 3020 surface area and porosity measur-

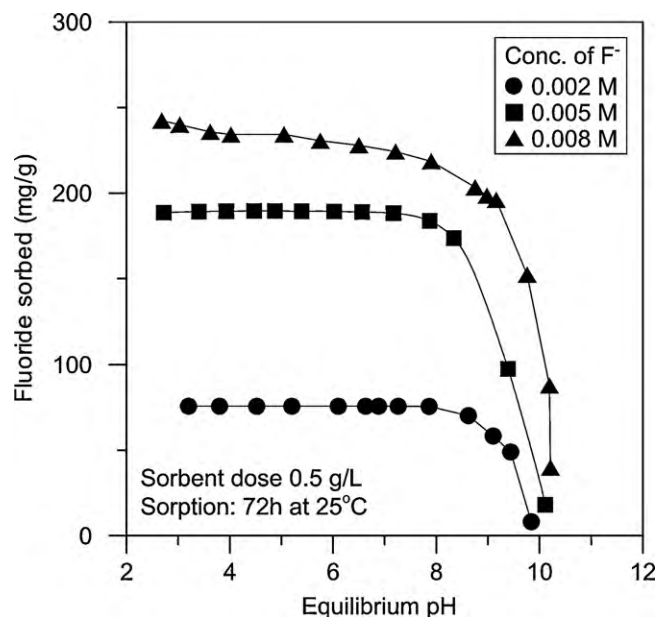


Fig. 1. Effect of pH on the defluoridation capacity of lanthanum hydroxide.

ing system (Micromeritics Instrument Co., USA) and a laser particle size analyzer (Mastersizer S, Malvern Instruments Ltd., UK), respectively. The mineral composition of the lanthanum hydroxide was characterized by X-ray diffractometer (X'pert-pro MPD, PANalytical, The Netherlands).

## 3. Results and discussion

### 3.1. Effect of pH on defluoridation

The effect of pH on the sorption of fluoride on the lanthanum hydroxide was examined at different initial fluoride concentrations ranging from 0.002 to 0.008 M and a constant dosage of sorbent of 0.5 g/L. The pH of solution was controlled to be 2.5–10.5 after the sorption equilibrium by adding HCl and NaOH solution. Fig. 1 shows the results of the equilibrium uptake of fluoride ion onto the lanthanum hydroxide as a function of the equilibrium pH of solution. As shown in Fig. 1, the equilibrium uptake of fluoride ion onto the lanthanum hydroxide slightly decreased at high initial fluoride concentration but remained nearly constant at low initial fluoride concentration with increasing the pH of solution up to 7.5–8.0. The maximum sorption pH range was broader at lower fluoride concentrations. This implies that some surface sites were saturated for higher surface loadings. When pH approached  $\text{pH}_{\text{pzc}}$  (8.7–8.8), fluoride sorption sharply decreased with the increase of pH regardless of the initial fluoride concentrations because the positively charged surface sites, which served as fluoride binding sites, significantly decreased with the increase in pH. At high pH, furthermore, it is also inferable that the competition between hydroxide ion ( $\text{OH}^-$ ) and fluoride ion ( $\text{F}^-$ ) limits the uptake efficiency. The results are in good agreement with the similar work done by other workers for granular ferric hydroxide [38]. They have reported that the mechanism of fluoride sorption on metal oxide surfaces can be described as an exchange reaction against  $\text{OH}^-$  of surface groups [39,40]. It is expected that similar process will occur on the lanthanum hydroxide. Thus, it is believed that ion-exchange reaction is a major mechanism for removal of fluoride ion by lanthanum hydroxide:



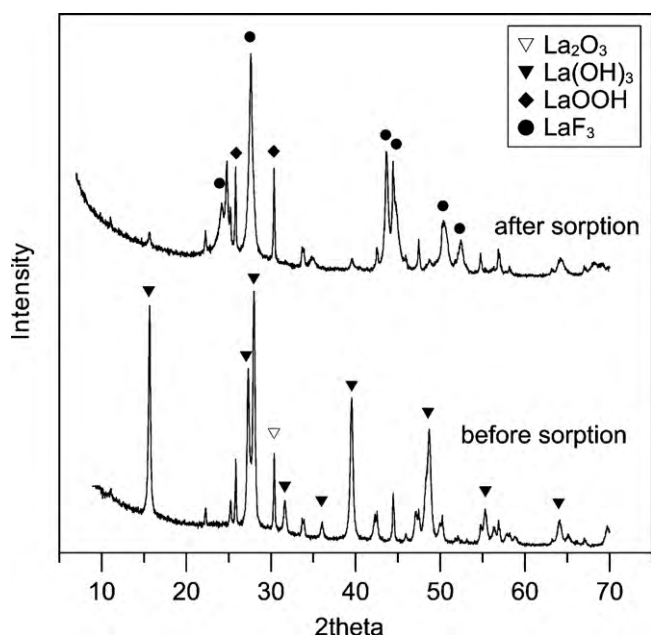


Fig. 2. XRD patterns of lanthanum hydroxide before and after fluoride sorption.



Experimental results show that the final pH was always higher than the initial pH, and the lower the pH, the more fluoride was removed from solution. The anion-exchange type defluoridation mechanism as suggested is consistent well with the observed increase of the final pH of solution (Eq. (2)) and increase of the defluoridation efficiency at low pH (Eq. (3)). Furthermore, as shown in Fig. 2, the XRD patterns show that the lanthanum hydroxide was converted into the lanthanum fluoride after the sorption of fluoride, and confirm that the exchange reaction between hydroxide ions of lanthanum hydroxide and fluoride ions in the solution occurred.

### 3.2. Effects of competing anions

One of the major problems which limit the wide application of sorption method to eliminate pollutants is the ion selectivity for a sorbent. Fig. 3 shows the effects of competing anions such as  $\text{Cl}^-$ ,  $\text{HCO}_3^-$ ,  $\text{NO}_3^-$ ,  $\text{HPO}_4^{2-}$ , and  $\text{SO}_4^{2-}$  on the uptake of fluoride ion onto the lanthanum hydroxide and the commercial PA resin. The experiments were conducted under a binary system, where contains 20 mg/L of fluoride ion paired with 0, 20, 50, and 100 mg/L of each competing anion. As shown in Fig. 3, it is obvious that the defluoridation capacity of lanthanum hydroxide was not influenced significantly by the presence of competing anions within the concentration range tested. On the contrary, the PA resin showed a significant decrease in uptake of fluoride ion as the concentration of competing anions increases. It was also found that defluoridation efficiencies of magnesia-amended activated alumina [41] and neodymium-modified chitosan [35] are not significantly affected by co-existing ions excepting bicarbonate.

From these results, it is obvious that lanthanum hydroxide has a high affinity for fluoride ion and there is no significant influence of competing anions on its defluoridation capacity, and hence that the lanthanum hydroxide can be used effectively as a fluoride selective sorbent.

### 3.3. Effect of sorbent dose

The effects of sorbent dose on the defluoridation efficiency at three different initial concentrations of fluoride in the solution were

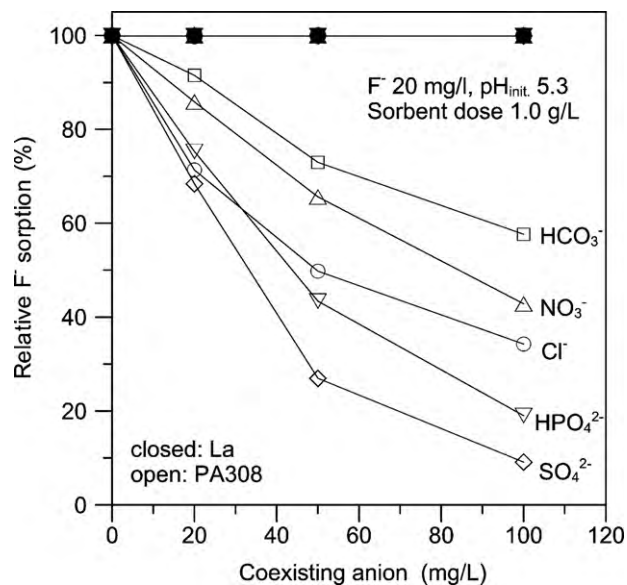


Fig. 3. Effect of competing anions on the defluoridation capacity of lanthanum hydroxide and PA resin.

shown in Fig. 4. It was observed that residual concentration of fluoride (Fig. 4(a)) and defluoridation capacity (Fig. 4(b)) decreased with the increase in sorbent dose; e.g., when the initial concentration of fluoride ions was 0.008 mol/L, the residual concentration of fluoride decreased from 123 to 0.83 mg/L with the increase in sorbent dose from 0.1 to 0.6 g/L; defluoridation capacity decreased from 290 to 251 mg/g. It was also found that the residual concentration of fluoride rapidly decreased up to a certain range in sorbent dose due to the increase in sorbent/sorbate ratio, however further increase in sorbent dose did not show any remarkable decrease in the residual concentration of fluoride. This may be because of the very low equilibrium concentration of fluoride ion, in which driving force responsible for sorption becomes negligible. The minimal dosages of the lanthanum hydroxide for reducing the residual fluoride ions to lower than 1.0 mg/L are found to be approximately 0.2, 0.4, and 0.6 g/L at 0.002, 0.005, and 0.008 mol/L of initial fluoride concentration, respectively.

### 3.4. Sorption isotherms

In order to study the sorption isotherm of the lanthanum hydroxide for fluoride, the lanthanum hydroxide of 0.05 g was contacted with the fluoride solution of 100 mL having concentrations in the range of 10–170 mg/L at two different initial pHs of 2.6 and 5.6. Each sample was allowed to equilibrate for 72 h at 25 °C, with constant shaking of 120 rpm, prior to analysis for the final fluoride ion concentration.

The experimental data obtained at different pH of solutions were plotted in a linearised form of Langmuir and Freundlich isotherm models as shown below:

$$\frac{C_e}{q_e} = \frac{1}{bq_m} + \frac{C_e}{q_m} \quad (4)$$

$$\ln q_e = \ln K_F + \frac{1}{n} \ln C_e \quad (5)$$

where  $C_e$  is the equilibrium concentration (mg/L),  $q_e$  is the amount sorbed at equilibrium (mg/g),  $q_m$  is the Langmuir constants related to the maximum monolayer sorption capacity (mg/g),  $b$  is an energy term (L/mg) which varies as a function of surface coverage strictly due to variations in the heat of adsorption,  $K_F$  and  $n$  are the Freundlich constants related to the sorption capacity of the sorbent and the magnitude of the sorption driving force, respec-

tively. The sorption data of fluoride on the lanthanum hydroxide selectively followed Langmuir and/or Freundlich isotherm models depending on the pH of solution as shown in Fig. 5. The calculated isotherm parameters along with regression coefficients are given in Table 1. The Langmuir isotherm model described the experimental data well regardless of the pH conditions of solution (Fig. 5(a)), indicating that fluoride is sorbed in the form of monolayer coverage on the surface of the lanthanum hydroxide. The maximum monolayer sorption capacity ( $q_m$ ) of the lanthanum hydroxide for fluoride is found to be 242.2 and 24.8 mg/g at  $\text{pH}_{\text{eq}} \leq 7.5$  and  $\text{pH}_{\text{eq}} > 10.0$ , respectively. The comparison of  $q_m$  values of the lanthanum hydroxide used in the present study with those reported in the literature shows that the lanthanum hydroxide is more effective for removal of fluoride ions, as shown in Table 2.

It was observed that the data obtained at high pH region ( $\text{pH}_{\text{eq}} > 10.0$ ) fitted well the Freundlich isotherm model, with the regression coefficient ( $r^2$ ) obtained higher than that obtained from the Langmuir isotherm model (Fig. 5(b)). However, the Freundlich model was not applicable to the isotherm data obtained at low pH region ( $\text{pH}_{\text{eq}} \leq 7.5$ ) due to low  $r^2$  value (Table 1). The suitability of Freundlich model in the isotherm data obtained at high pH region is the indication of a multilayer sorption and heterogeneous nature of the sorbent surface. It may be due to the increase of competition of hydroxide ions with fluoride for sorption sites and negatively charged surface sites on the sorbent at high pH condition of solution. Nevertheless, the magnitude of  $n$  value related to the sorption driving force was in level of a favorable sorption process. Furthermore, high  $n$  value ( $n > 1$ ) indicates that the sorption driving force is favorable at high concentrations but much less at lower concentrations [46,47].

### 3.5. Sorption kinetics

Fig. 6 shows the plots of fluoride sorption kinetic data obtained at three different initial concentrations and at 25 °C on the lanthanum hydroxide. It was obvious that the time required for reaching equilibrium has increased with increasing the concentration of fluoride and that has been found to be 4 h for the lowest concentration (0.002 mol/L) while greater than 72 h for the highest concentration (0.008 mol/L) studied. Fig. 7 shows the fluoride sorption kinetic data obtained at three different temperatures with a

fluoride concentration of 0.008 mol/L. The time required for reaching equilibrium has reduced from  $\geq 72$  h to  $\leq 16$  h with the increase of temperature from 25 to 45 °C, which indicates an endothermic nature of the sorption process.

In order to interpret the experimental data, the time-dependent sorption data have been analyzed using the linear form of the pseudo-first-order kinetic equation and pseudo-second-order kinetic equation.

The pseudo-first-order kinetic model of Lagergren is given as [48]:

$$\ln(q_e - q_t) = \ln q_e - k_1 t \quad (6)$$

where  $q_e$  and  $q_t$  are the amount of adsorbate adsorbed at equilibrium and time  $t$  (mg/g), respectively, and  $k_1$  is the rate constant of pseudo-first-order adsorption ( $\text{min}^{-1}$ ). Fig. 8 shows a plot of linearised form of the pseudo-first-order kinetic model using the sorption data of Fig. 6. Only the first portion of sorption kinetics gives a straight fitting line, indicating that the pseudo-first-order kinetic model cannot be used to predict the defluoridation kinetics of lanthanum hydroxide over the entire sorption period. The values of  $k_1$  and  $q_e$ , and the regression coefficients evaluated from the first linear portions are presented in Table 3. As shown in Table 3, the regression coefficients for the first-order-kinetic model obtained at all the studied concentrations were relatively high ( $r^2 > 0.98$ ). However, although  $r^2$  values are reasonably high, the calculated  $q_e$  values obtained from this equation do not give reasonable values, which are too low compared with experimental  $q_e$  values. In addition, it was observed that, at all initial fluoride concentrations studied, the sorption data were well represented by the pseudo-first-order kinetic model only for the first 240 or 480 min and thereafter they deviated from the theory. This suggests that the sorption process does not follow the pseudo-first-order kinetic model.

The pseudo-second-order kinetic equation, which is more likely to predict the behavior over entire sorption period and is in agreement with chemical sorption being the rate-controlling step, is given as [49]:

$$\frac{t}{q_t} = \frac{1}{k_2 q_e^2} + \frac{t}{q_e} \quad (7)$$

**Table 1**  
Langmuir and Freundlich isotherm parameters.

pH of solution	Langmuir isotherm			Freundlich isotherm		
	$q_m$ (mg/g)	$b$ (L/mg)	$r^2$	$K_F$ (mg/g)(L/mg) $^{1/n}$	$n$	$r^2$
$\text{pH}_{\text{eq}} \leq 7.5$	242.2	4.509	0.999	111.31	4.13	0.596
$\text{pH}_{\text{eq}} > 10.0$	24.8	0.022	0.965	2.16	2.34	0.987

**Table 2**  
Comparative assessment of Langmuir monolayer sorption capacity of lanthanum hydroxide with some literature available data for other adsorbents.

Adsorbent	$q_m$ (mg/g)	Experimental conditions	Reference
Montmorillonite	3.37	pH 6.0, $C_0$ : 2–120 mg/L	[8]
Activated alumina	2.41	pH 7.0, $C_0$ : 2.5–14 mg/L	[19]
Hydroxyapatite	4.54	pH 6.0, $C_0$ : $2.5 \times 10^{-5}$ to $6.34 \times 10^{-2}$ mol/L	[21]
KMnO <sub>4</sub> -modified carbon	15.90	pH 2.0, $C_0$ : 5–20 mg/L	[22]
Quick lime	16.67	pH 6.61, $C_0$ : 10–50 mg/L	[24]
Granular ferric hydroxide	5.97	pH 6.0–7.0, $C_0$ : 1–100 mg/L	[38]
Iron-zirconium hybrid oxide	8.21	pH 6.8 ± 0.1, $C_0$ : 5–50 mg/L	[42]
Iron-aluminum mixed oxide	17.73	pH 6.9 ± 0.2, $C_0$ : 10–50 mg/L	[43]
Iron-tin mixed oxide	10.47	pH 6.4 ± 0.2, $C_0$ : 10–50 mg/L	[44]
Magnetic-chitosan	22.49	pH 7.0, $C_0$ : 5–40 mg/L	[45]
Nd-modified chitosan	22.38	pH 7.0, $C_0$ : 10–100 mg/L	[35]
La-modified chitosan	11.90	pH 7.0, $C_0$ : 10–20 mg/L	[36]
Lanthanum hydroxide	242.20	$\text{pH}_{\text{eq}} \leq 7.5$ ( $\text{pH}_{\text{init}}$ : 2.6), $C_0$ : 10–150 mg/L	This study
	24.80	$\text{pH}_{\text{eq}} > 10.0$ ( $\text{pH}_{\text{init}}$ : 5.6), $C_0$ : 10–170 mg/L	



**Table 3**  
First- and second-order kinetic parameters.

$C_0$ (mol/L)	Experiment $q_e$ (mg/g)	Pseudo-first-order kinetics <sup>a</sup>			Pseudo-second-order kinetics		
		$k_1$ ( $\text{min}^{-1}$ )	$q_e$ (mg/g)	$r^2$	$k_2$ (g/mg min)	$q_e$ (mg/g)	$r^2$
0.002	75.4	$2.13 \times 10^{-2}$	120.9	0.986	$5.97 \times 10^{-3}$	75.5	1.000
0.005	172.8	$2.25 \times 10^{-3}$	145.9	0.999	$3.74 \times 10^{-5}$	173.2	0.999
0.008	237.3	$1.13 \times 10^{-3}$	220.3	0.985	$1.31 \times 10^{-5}$	246.4	0.999

<sup>a</sup> Only for initial sorption period (0–240 min for 0.002 mol/L, 0–480 min for 0.005 and 0.008 mol/L).

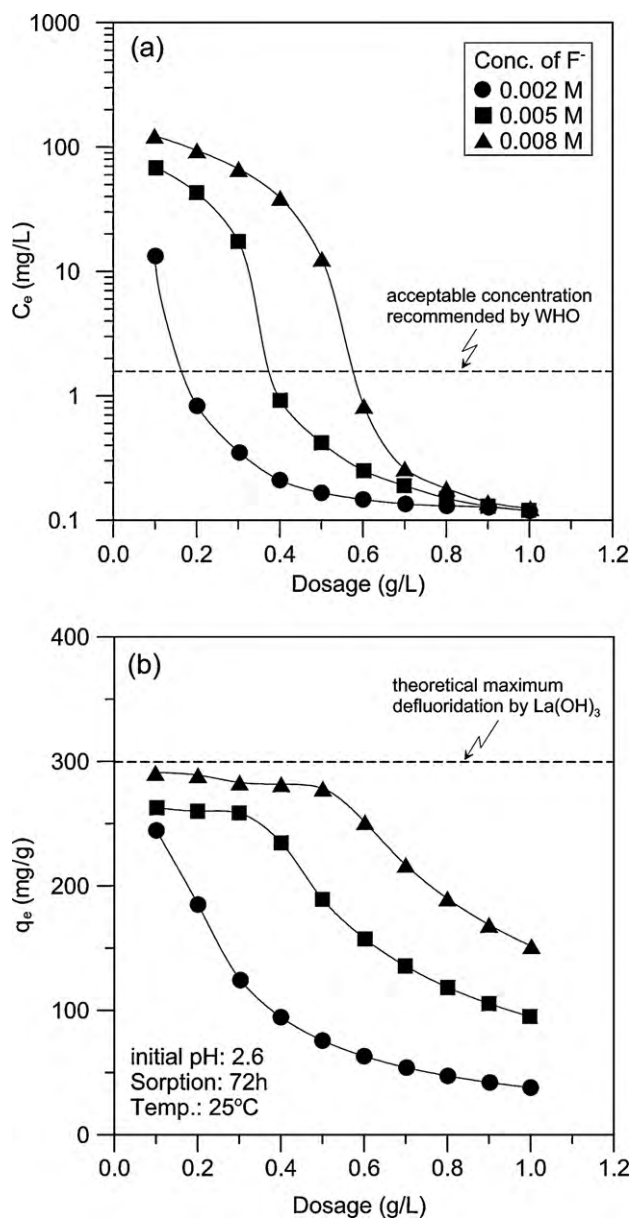


**Fig. 4.** Effect of sorbent dose on the defluoridation of lanthanum hydroxide: (a) equilibrium concentration and (b) defluoridation capacity.

where  $q_e$  and  $q_t$  are the amount (mg/g) of adsorbate adsorbed at equilibrium and time  $t$ , respectively, and  $k_2$  is the rate constant of pseudo-second-order adsorption (g/mg min). Fig. 9 shows the linear plots of the pseudo-second-order equation using the data of Fig. 6. The plots were found to be linear over the entire sorption period with good regression coefficients ( $r^2 > 0.99$ ), confirming the applicability of the pseudo-second-order kinetic model. The pseudo-second-order rate constant ( $k_2$ ) and equilibrium capacity ( $q_e$ ) determined from the slopes and intercepts of the plots (Fig. 9

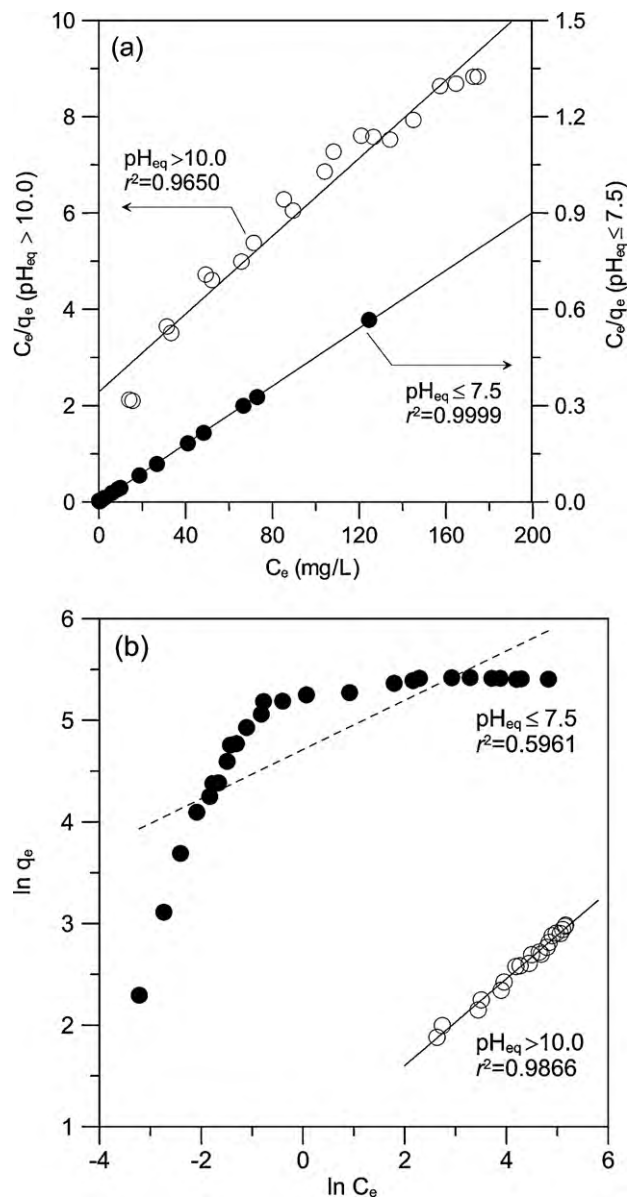


**Fig. 5.** Langmuir (a) and Freundlich (b) isotherm plots of fluoride sorption on lanthanum hydroxide.

are listed in Table 3. The regression coefficients for the linear plots of  $t/q_t$  against  $t$  for the second-order kinetic equation were observed to be close to unity for the contact time of 72 h. The theoretical  $q_e$  values for the fluoride–lanthanum hydroxide system were also very close to the experimental  $q_e$  values in the case of the pseudo-second-order kinetic equation (Table 3). It is clear from the accuracy of the model that the sorption of fluoride on the lanthanum hydroxide is more appropriately described by the pseudo-second-order kinetic model. The confirmation of pseudo-second-order kinetics

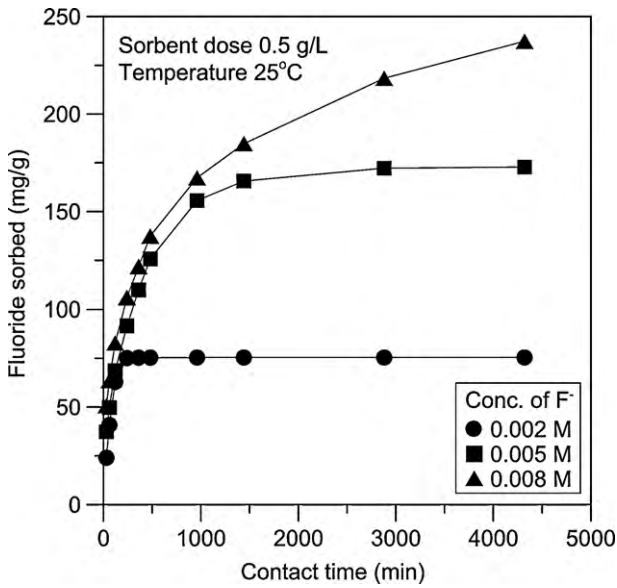


Fig. 6. Effect of initial concentration to sorption rate of fluoride on lanthanum hydroxide.

indicates that in the sorption process, concentrations of both sorbate and sorbent are involved in rate-determining step, which may be a chemical sorption or chemisorption [50]. The results showed the decrease of  $k_2$  values but the increase of  $q_e$  values with increasing initial fluoride concentration (Table 3). Thus, the rate of sorption decreases with increasing solute concentrations, which is similar to the results from various sorbents reported by other workers [51,52].

### 3.6. Sorption thermodynamics

The experimental data obtained at different temperatures in the range of 25–45 °C were used in calculating the thermodynamic parameters of fluoride sorption using the lanthanum hydroxide. The standard enthalpy change ( $\Delta H^\circ$ ), standard entropy change ( $\Delta S^\circ$ ) and Gibbs free energy change ( $\Delta G^\circ$ ) were calculated using

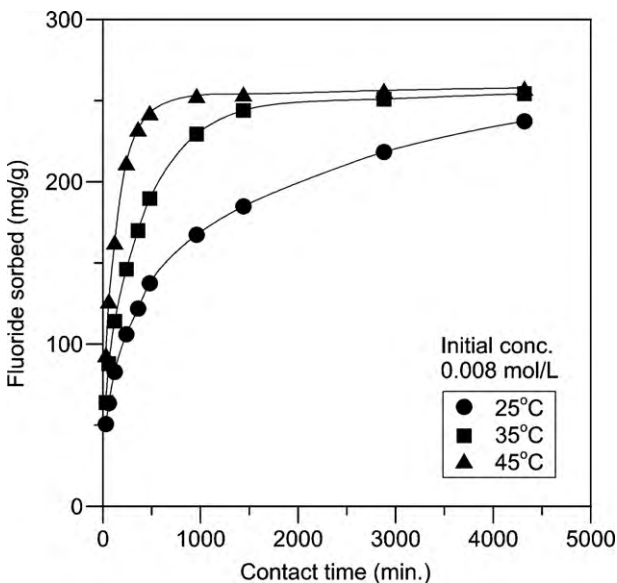


Fig. 7. Effect of temperature to sorption rate of fluoride on lanthanum hydroxide.

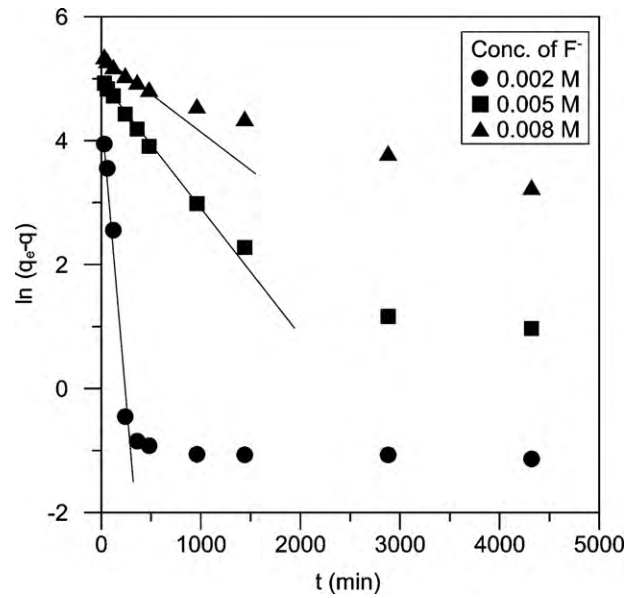


Fig. 8. Pseudo-first-order kinetic plot for fluoride sorption on lanthanum hydroxide.

following equations:

$$\ln b_M = \frac{\Delta S^\circ}{R} - \frac{\Delta H^\circ}{RT} \quad (8)$$

$$\Delta G^\circ = \Delta H^\circ - T\Delta S^\circ \quad (9)$$

where  $b_M$  is the Langmuir constant (L/mol) that relates to the energy of sorption,  $R$  is the universal gas constant (kJ/mol K), and  $T$  is the temperature (K). The plots of  $\ln b_M$  versus  $1/T$  are shown in Fig. 10. The values of  $\Delta H^\circ$  and  $\Delta S^\circ$  for fluoride sorption were calculated from the slope and intercept of the plot, respectively, by regression analysis. The values of  $\Delta G^\circ$  were calculated using Eq. (9). Thermodynamic parameters for the sorption of fluoride on the lanthanum hydroxide are given in Table 4. As shown in Fig. 10, the plot of  $\ln b_M$  versus  $1/T$  was found to be roughly linear but the regression coefficient was too low ( $r^2 < 0.81$ ) to determine exactly the thermodynamic parameters using the slope and intercept of the regression line. As an alternative, therefore, the distribution coeffi-

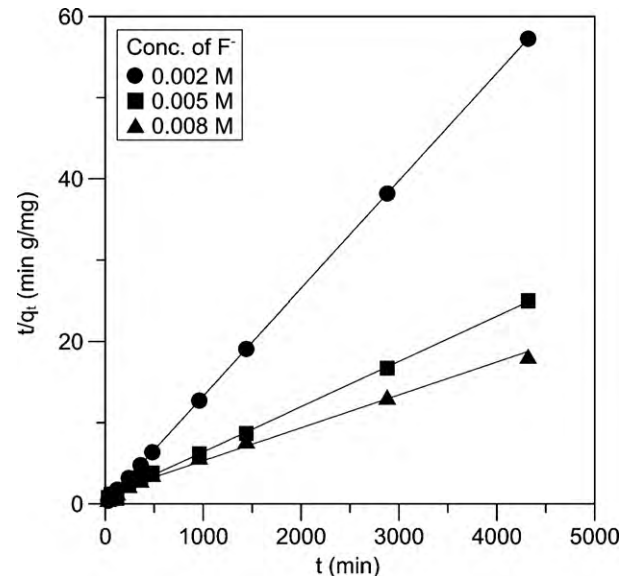


Fig. 9. Pseudo-second-order kinetic plot for fluoride sorption on lanthanum hydroxide.

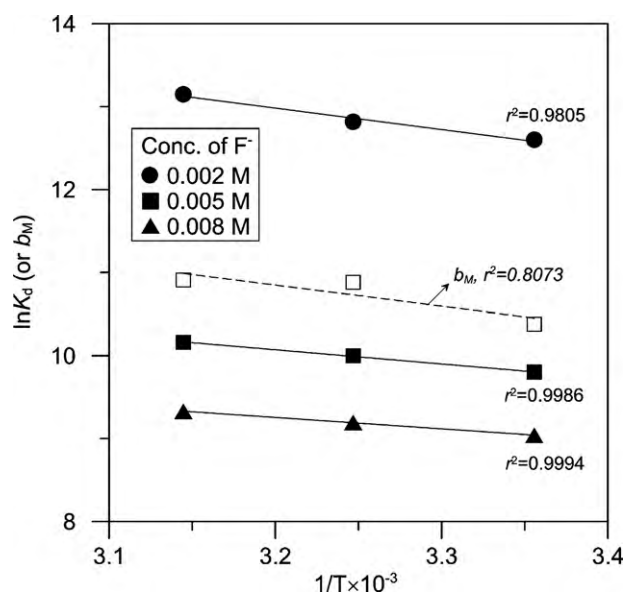


Fig. 10. Plot of  $\ln K_d$  versus  $1/T$  for fluoride sorption on lanthanum hydroxide.

cient ( $K_d$ ) was used for evaluating the thermodynamic parameters instead of the Langmuir constant  $b_M$ .  $K_d$  is approximated here as an empirical equilibrium constant defined as  $C_{Ae}/C_e$  at a particular initial concentration.  $C_{Ae}$  (mg/kg) is the amount adsorbed on solid at equilibrium. The plots of  $\ln K_d$  versus  $1/T$  are shown in Fig. 10 and the thermodynamic parameters evaluated are given in Table 4. The evaluation of the thermodynamic parameters by using  $K_d$  is subject to a number of limitations. One of the most important limitations is the fact that the  $K_d$  is not a thermodynamic equilibrium constant but merely an empirical constant that is valid under a particular set of reaction conditions. The dependence of  $K_d$  on the initial concentration is thus reflected in the calculated  $\Delta H^\circ$ ,  $\Delta S^\circ$ , and  $\Delta G^\circ$  values. Nevertheless, the thermodynamic parameters evaluated systematically varied with the initial concentration within a narrow range and roughly corresponded to those evaluated using  $b_M$  as shown in Table 4. This result suggests the availability of  $K_d$  for the sorption thermodynamic study. The positive value of  $\Delta H^\circ$  demonstrates that the sorption process is of endothermic nature. This behavior indicates that higher temperatures are more preferred for higher fluoride sorption. The positive value of  $\Delta S^\circ$  shows increased disorder at the solid–solution interface during the sorption of fluoride. The sorption increases randomness at the solid–solution interface with some structural changes in the sorbate and sorbent and an affinity of the sorbent toward fluoride. Similar results for endothermic sorption of fluoride were also observed on granular ferric hydroxide [38], hydrous iron(III)–tin(IV) bimetal mixed oxide [44],  $\text{Na}^+$  or  $\text{Al}^{3+}$ -incorporated ion-exchange resin [53], and protonated chitosan beads [54]. The negative values of  $\Delta G^\circ$  at all temperatures indicate that the sorption of fluoride onto lanthanum hydroxide is spontaneous and thermodynamically favorable. The more nega-

Table 4  
Thermodynamic parameters for sorption of fluoride on lanthanum hydroxide.

$C_0$ (mol/L)	$\Delta H^\circ$ (kJ/mol)	$\Delta S^\circ$ (J/molK)	$\Delta G^\circ$ (kJ/mol) at studied temperature			$E_a$ (kJ/mol)
			25 °C	35 °C	45 °C	
0.001–0.01 <sup>a</sup>	21.07	157.62	–25.71 <sup>b</sup>	–26.96 <sup>b</sup>	–27.03 <sup>b</sup>	
0.002	21.52	176.80	–31.17	–32.05	–33.82	53.40
0.005	14.24	129.30	–24.30	–24.94	–26.23	65.34
0.008	11.39	113.41	–22.40	–22.97	–24.10	68.67

<sup>a</sup> Langmuir constant,  $b_M$ , was used as the thermodynamic equilibrium constant.

<sup>b</sup> directly calculated by using  $\Delta G^\circ = -RT \ln b_M$ .

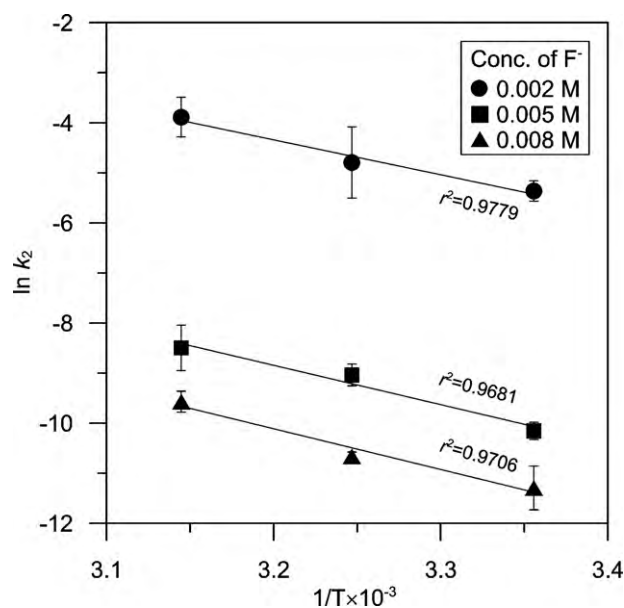


Fig. 11. Arrhenius plot for fluoride sorption on lanthanum hydroxide.

tive the  $\Delta G^\circ$ , the stronger the driving force of adsorption reaction. The decrease in the value of  $\Delta G^\circ$  with the increase of temperature shows that the reaction is more spontaneous at high temperature which indicates that the sorption processes are favored by the increase in temperature [55].

Finally, Arrhenius equation has been applied to evaluate the activation energy of fluoride sorption representing the minimum energy that reactants must have for the reaction to proceed, as shown by the following relationship [56]:

$$\ln k_2 = \ln A - \frac{E_a}{RT} \quad (11)$$

where  $A$  is the temperature-independent factor (g/mg min),  $k_2$  is the pseudo-second-order rate constant value for the ions sorption,  $E_a$  is the activation energy in kJ/mol. As shown in Fig. 11, the plots of  $\ln k_2$  versus  $1/T$  were found to be linear with acceptable regression coefficient values  $r^2$  for all temperatures and initial fluoride concentrations studied. The activation energies for the sorption system studied were derived from the slopes of the plots and were calculated to be 53.4–68.8 kJ/mol, and tended to increase with increasing the initial fluoride concentration in the solution (Table 4). The magnitude of activation energy gives an idea about the type of sorption which is mainly physical or chemical. Low activation energies are characteristics for physical sorption, while higher activation energies suggest chemical sorption [57]. It is known that the activation energy for physical sorption is usually  $\leq 4.2$  kJ/mol. An activated chemical sorption means that the rate varies with temperature according to the finite activation energy (8.4–83.7 kJ/mol) in the Arrhenius equation [58]. In non-activated chemical sorption, the activation energy is near zero [59]. The activation energies obtained

were of the same magnitude as that of activated chemical sorption. The positive values of  $E_a$  also suggest that an increase in temperature favors the fluoride sorption onto the lanthanum hydroxide and the sorption process is an endothermic in nature.

### 3.7. Desorption study

In order to assess the possibility of recycling the sorbent for reuse in multiple sorption cycle, fluoride desorption experiments for the used lanthanum hydroxide were conducted using NaOH solution with various concentrations in the range of 0.1–2.0 M. It was found that fluoride desorption was 24.9, 43.2, 70.9, 86.3, 89.6 and 89.7% with 0.1, 0.2, 0.5, 1.0, 1.5 and 2.0 M NaOH, respectively, when 100 mL fractions of NaOH solution per g fluoride-loaded lanthanum hydroxide are added and shaken for 1 h at 25 °C. The results indicated that the optimum concentration of NaOH for fluoride desorption is 1.0 M in terms of economical process. Although further work should be performed systematically to optimize the regeneration system, it may be concluded that the fluoride-loaded lanthanum hydroxide undergoes effective desorption in the presence of electrolyte like NaOH.

## 4. Conclusions

The defluoridation capacity of lanthanum hydroxide remained nearly constant up to  $\text{pH}_{\text{eq}}$  7.5–8.0, and thereafter sharply decreased with increasing the pH of solution. The  $\text{pH}_{\text{PZC}}$  was approximately 8.75 ( $\pm 0.05$ ) for this material. The co-existing anions,  $\text{Cl}^-$ ,  $\text{HCO}_3^-$ ,  $\text{NO}_3^-$ ,  $\text{HPO}_4^{2-}$  and  $\text{SO}_4^{2-}$ , showed no adverse effect on the fluoride removal by the lanthanum hydroxide. The equilibrium data fairly well fitted the Langmuir isotherm model, and the maximum monolayer sorption capacity was found to be 242.2 mg/g at  $\text{pH}_{\text{eq}} \leq 7.5$  and 24.8 mg/g at  $\text{pH}_{\text{eq}} > 10.0$ . The sorption process followed the pseudo-second-order kinetic model. Thermodynamic parameters such as  $\Delta G^\circ$ ,  $\Delta H^\circ$  and  $\Delta S^\circ$  indicate that the nature of fluoride sorption is spontaneous and endothermic. The activation energy,  $E_a$  for defluoridation of lanthanum hydroxide was found to be 53.4–68.8 kJ/mol indicating an activated chemical sorption process and increased with increasing the initial fluoride concentration. The used lanthanum hydroxide could be regenerated with NaOH solution where 86% of the sorbed fluoride was desorbed by 1.0 M NaOH. The results demonstrate that the lanthanum hydroxide can be effectively used for removal of fluoride from aqueous solutions with a good selectivity.

## Acknowledgements

This work was supported by the annex laboratory project funded by the Korean Small and Medium Business Administration (SMBA).

## References

- [1] D. Banks, C. Reimann, O. Røyset, H. Skarphagen, O.M. Saether, Natural concentrations of major and trace elements in some Norwegian bedrock groundwaters, *Appl. Geochem.* 10 (1995) 1–16.
- [2] F. Shen, X. Chen, P. Gao, G. Chen, Electrochemical removal of fluoride ions from industrial wastewater, *Chem. Eng. Sci.* 58 (2003) 987–993.
- [3] G. Puente, J.J. Pis, J.A. Menendez, P. Grange, Thermal stability of oxygenated functions in activated carbons, *J. Anal. Appl. Pyrol.* 43 (1997) 125–138.
- [4] N.J. Chinoy, Effects of fluoride on physiology of animals and human beings, *Indian J. Environ. Toxicol.* 1 (1991) 17–32.
- [5] P.T.C. Harrison, Fluoride in water: a UK perspective, *J. Fluor. Chem.* 126 (2005) 1448–1456.
- [6] WHO, Guidelines for Drinking Water Quality, vol. 1(1), World Health Organization, Geneva, 1993, pp. 45–46.
- [7] USEPA, National Primary Drinking Water Standard, EPA 816-F-03-016, 2003.
- [8] A. Tor, Removal of fluoride from an aqueous solution by using montmorillonite, *Desalination* 201 (2006) 267–276.
- [9] X. Wu, Y. Zhang, X. Dou, M. Yang, Fluoride removal performance of a novel Fe–Al–Ce trimetal oxide adsorbent, *Chemosphere* 69 (2007) 1758–1764.
- [10] S. Ayoob, A.K. Gupta, Sorptive response profile of an adsorbent in the defluoridation of drinking water, *Chem. Eng. J.* 133 (2007) 273–281.
- [11] S.S. Tripathy, J. Bersillon, K. Gopal, Removal of fluoride from drinking water by adsorption onto alum-impregnated activated alumina, *Sep. Purif. Technol.* 50 (2006) 310–317.
- [12] S. Meenakshi, N. Viswanathan, Identification of selective ion-exchange resin for fluoride sorption, *J. Colloid Interface Sci.* 308 (2007) 438–450.
- [13] G. Chae, S. Yun, B. Mayer, K. Kim, S. Kim, J. Kwon, K. Kim, Y. Koh, Fluorine geochemistry in bedrock groundwater of South Korea, *Sci. Total Environ.* 385 (2007) 272–283.
- [14] J. Zhu, H. Zhao, J. Ni, Fluoride distribution in electrocoagulation defluoridation process, *Sep. Purif. Technol.* 56 (2007) 184–191.
- [15] R. Simons, Trace element removal from ash dam waters by nanofiltration and diffusion dialysis, *Desalination* 89 (1993) 325–341.
- [16] E. Kir, E. Alkan, Fluoride removal by Donnan dialysis with plasma-modified and unmodified anion-exchange membranes, *Desalination* 197 (2006) 217–224.
- [17] M. Tahaik, R. El Habbani, A. Ait Haddou, I. Achary, Z. Amor, M. Taky, A. Alamib, A. Boughriba, M. Hafsi, A. Elmidaoui, Fluoride removal from groundwater by nanofiltration, *Desalination* 212 (2007) 46–53.
- [18] M. Tahaik, I. Achary, M.A. Menkouchi Sahli, Z. Amor, M. Taky, A. Alami, A. Boughriba, M. Hafsi, A. Elmidaoui, Defluoridation of Moroccan ground water by electro-dialysis: continuous operation, *Desalination* 167 (2004) 357–365.
- [19] S. Ghorai, K.K. Pant, Investigation on the column performance of fluoride adsorption by activated alumina in a fixed bed, *Chem. Eng. J.* 98 (2004) 165–173.
- [20] S. Meenakshi, C. Sairam Sundaram, R. Sukumar, Enhanced fluoride sorption by mechanochemically activated kaolinites, *J. Hazard. Mater.* 153 (2008) 164–172.
- [21] X. Fan, D.J. Parker, M.D. Smith, Adsorption kinetics of fluoride on low cost materials, *Water Res.* 37 (2003) 4929–4937.
- [22] A.A.M. Daifullah, S.M. Yakout, S.A. Elreefy, Adsorption of fluoride in aqueous solutions using  $\text{KMnO}_4$ -modified activated carbon derived from steam pyrolysis of rice straw, *J. Hazard. Mater.* 147 (2007) 633–643.
- [23] S. Meenakshi, N. Viswanathan, Identification of selective ion exchange resin for fluoride sorption, *J. Colloid Interface Sci.* 308 (2007) 438–450.
- [24] M. Islam, R.K. Patel, Evaluation of removal efficiency of fluoride from aqueous solution using quick-lime, *J. Hazard. Mater.* 143 (2007) 303–310.
- [25] R. Piekos, S. Paslawaska, Fluoride uptake characteristic of fly ash, *Fluoride* 32 (1999) 14–19.
- [26] Y. Cengeloglu, E. Kir, M. Ersoz, Removal of fluoride from aqueous solution by using red mud, *Sep. Purif. Technol.* 28 (2002) 81–86.
- [27] D. Mohapatra, D. Mishra, S.P. Mishra, G. Roychaudhary, R.P. Das, Use of oxide minerals to abate fluoride from water, *J. Colloid Interface Sci.* 275 (2004) 355–359.
- [28] N. Das, P. Pattanaik, R. Das, Defluoridation of drinking water using activated titanium rich bauxite, *J. Colloid Interface Sci.* 292 (2005) 1–10.
- [29] M. Sarkar, A. Banerjee, P.P. Pramanik, A.R. Sarkar, Use of laterite for the removal of fluoride from contaminated drinking water, *J. Colloid Interface Sci.* 302 (2006) 432–444.
- [30] M.G. Sujana, H.K. Pradhan, S. Anand, Studies on sorption of some geomaterials for fluoride removal from aqueous solutions, *J. Hazard. Mater.* 161 (2009) 120–125.
- [31] A.S. Wasay, Md.J. Haron, S. Tokunaga, Adsorption of fluoride, phosphate and arsenate ions on lanthanum impregnated silica gel, *Water Environ. Res.* 68 (1996) 295–300.
- [32] S.A. Wasay, S. Tokunaga, S.W. Park, Removal of hazardous anions from aqueous solutions by La(III)- and Y(III)-impregnated alumina, *Sep. Sci. Technol.* 31 (1991) 1501–1514.
- [33] Y.M. Zhou, C.X. Yu, Y. Shan, Adsorption of fluoride from aqueous solution on  $\text{La}^{3+}$ -impregnated cross-linked gelatin, *Sep. Purif. Technol.* 36 (2004) 89–94.
- [34] R.X. Li, H.X. Tang, Adsorptive properties of fluoride ion on lanthanum-loaded fibrous sorbent, *Environ. Sci.* 21 (2000) 34–37.
- [35] R. Yao, F. Meng, L. Zhang, D. Ma, M. Wang, Defluoridation of water using neodymium-modified chitosan, *J. Hazard. Mater.* 165 (2009) 454–460.
- [36] N. Viswanathan, S. Meenakshi, Enhanced fluoride sorption using La(III) incorporated carboxylated chitosan beads, *J. Colloid Interface Sci.* 322 (2008) 375–383.
- [37] J.A. Schwarz, C.T. Driscoll, A.K. Bhanot, The zero point charge of silica–alumina oxide suspension, *J. Colloid Interface Sci.* 97 (1984) 55–61.
- [38] E. Kumar, A. Bhatnagar, M. Ji, W. Jung, S.-H. Lee, S.-J. Kim, G. Lee, H. Song, J.-Y. Choi, J.-S. Yang, B.-H. Jeon, Defluoridation from aqueous solutions by granular ferric hydroxide (GFH), *Water Res.* 43 (2009) 490–498.
- [39] J.C.L. Meeussen, A. Scheidegger, T. Hiemstra, W.H. van Riemsdijk, M. Borkovec, Predicting multi-component adsorption and transport of fluoride at variable pH in a goethite–silica sand system, *Environ. Sci. Technol.* 30 (1996) 481–488.
- [40] T. Hiemstra, W.H. van Riemsdijk, Fluoride adsorption on goethite in relation to different types of surface sites, *J. Colloid Interface Sci.* 225 (2000) 94–104.
- [41] S.M. Maliyekkal, S. Shukla, L. Philip, I.M. Nambi, Enhanced fluoride removal from drinking water by magnesia-amended activated alumina granules, *Chem. Eng. J.* 140 (2008) 183–192.
- [42] K. Biswas, D. Bandhoyapadhyay, U.C. Ghosh, Adsorption kinetics of fluoride on iron(III)–zirconium(IV) hybrid oxide, *Adsorption* 13 (2007) 83–94.
- [43] K. Biswas, S.K. Saha, U.C. Ghosh, Adsorption of fluoride from aqueous solution by a synthetic iron(III)–aluminum(III) mixed oxide, *Ind. Eng. Chem. Res.* 46 (2007) 5346–5356.
- [44] K. Biswas, K. Gupta, U.C. Ghosh, Adsorption of fluoride by hydrous iron(III)–tin(IV) bimetal mixed oxide from the aqueous solutions, *Chem. Eng. J.* 149 (2009) 196–206.



- [45] W. Ma, F.-Q. Ya, M. Han, R. Wang, Characteristic of equilibrium kinetics studies for the adsorption of fluoride on magnetic-chitosan particle, *J. Hazard. Mater.* 143 (2007) 296–302.
- [46] G. McKay, The removal of color from effluent using various adsorbents—IV silica, *Water Res.* 14 (1980) 1–27.
- [47] F.H. Frimmel, L. Huber, Influence of humic substances on the aquatic sorption of heavy metals on defined minerals phases, *Environ. Int.* 22 (1996) 507–517.
- [48] S. Lagergren, About the theory of so-called adsorption of soluble substances, *K. Sven. Ventenskasakad. Handl.* 24 (1898) 1–39.
- [49] Y.S. Ho, G. McKay, Pseudo-second order model for sorption process, *Process Biochem.* 34 (1999) 451–465.
- [50] Y.S. Ho, G. McKay, Comparisons of chemisorption kinetic models applied to pollutant removal on various sorbents, *Trans. Inst. Chem. Eng. B* 76 (1998) 332–340.
- [51] W. Li, L. Zhang, J. Peng, N. Li, S. Zhang, S. Guo, Tobacco stems as a low cost adsorbent for the removal of Pb(II) from wastewater: equilibrium and kinetic studies, *Ind. Crop. Prod.* 28 (2008) 294–302.
- [52] O. Hamdaoui, F. Saoudi, M. Chiha, E. Naffrechoux, Sorption of malachite green by a novel sorbent, dead leaves of plane tree: equilibrium and kinetic modeling, *Chem. Eng. J.* 143 (2008) 73–84.
- [53] N. Viswanathan, S. Meenakshi, Role of metal ion incorporation in ion exchange resin on the selectivity of fluoride, *J. Hazard. Mater.* 162 (2009) 920–930.
- [54] N. Viswanathan, C. Sairam Sundaram, S. Meenakshi, Removal of fluoride from aqueous solution using protonated chitosan beads, *J. Hazard. Mater.* 161 (2009) 423–430.
- [55] M. Syed, I. Muhammad, G. Rana, K. Sadullah, Effect of Ni<sup>2+</sup> loading on the mechanism of phosphate anion sorption by iron hydroxide, *Sep. Purif. Technol.* 59 (2008) 108–114.
- [56] J.M. Smith, *Chemical Engineering Kinetics*, 3rd ed., McGraw-Hill, Singapore, 1981.
- [57] H. Nollet, M. Roels, P. Lutgen, P. Van der Meeren, W. Verstraete, Removal of PCBs from wastewater using fly ash, *Chemosphere* 53 (2003) 655–665.
- [58] W. Zou, R. Han, Z. Chen, Z. Jinghua, J. Shi, Kinetic study of adsorption of Cu(II) and Pb(II) from aqueous solutions using manganese oxide coated zeolite in batch mode, *Colloids Surf. A: Physicochem. Eng. Aspects* 279 (2006) 238–246.
- [59] Z. Aksu, Determination of the equilibrium, kinetic and thermodynamic parameters of the batch biosorption of lead(II) ions onto *Chlorella vulgaris*, *Process Biochem.* 38 (2002) 89–99.